

# Isotope shift in the electron affinity of chlorine

Uldis Berzinsh, Morgan Gustafsson, Dag Hanstorp,  
Andreas E. Klinkmüller, Ulric Ljungblad  
and Ann-Maire Mårtensson-Pendrill

Department of Physics, Chalmers University of Technology  
and Göteborg University,  
SE 412 96 Göteborg, Sweden

14 July 1994

The specific mass shift in the electron affinity between  $^{35}\text{Cl}$  and  $^{37}\text{Cl}$  has been determined by tunable laser photodetachment spectroscopy to be  $-0.51(14)$  GHz. The isotope shift was observed as a difference in the onset of the photodetachment process for the two isotopes. In addition, the electron affinity of Cl was found to be  $29\,138.59(22)$   $\text{cm}^{-1}$ , giving a factor of 2 improvement in the accuracy over earlier measurements. Many-body calculations including lowest-order correlation effects demonstrates the sensitivity of the specific mass shift and show that the inclusion of higher-order correlation effects would be necessary for a quantitative description.

PACS number: 35.10.Hn, 32.80.Fb,  
31.30.Gs

## 1 Introduction

Tunable laser photodetachment spectroscopy makes high-resolution studies

of electron affinities possible, and in this work we demonstrated an application of this technique to the measurement of the isotope shift in the electron affinity of chlorine. The observed shift is only a fraction of the *normal mass shift* (NMS), indicating a *specific mass shift* (SMS) comparable to the normal mass shift, but of opposite sign. The results obtained provide a sensitive probe of electron correlation effects, which are known to be particularly important for negative ions and the specific mass shift.

The outermost electron in a negative ion is very weakly bound: Far from the nucleus it is bound only due to polarization of the other electrons in the system, whereas the outermost electron in an atom or positive ion is bound in a long-range Coulomb potential. Hence the electron correlation is of greater importance in negative ions, which therefore provide good tests of computational methods used to describe electron correlation. In  $\text{Li}^-$ , e. g., the electron

correlation energy has been found to be three times larger than the electron affinity [1]. Another system where the electron correlation is dominating the binding energy is the two-electron system  $\text{H}^-$ , which has been used as a model case in many calculations [2–4].

The specific mass shift arises from a correlation between the electronic momenta through the motion of the nucleus with its finite mass, and is discussed in more detail in section 3.1. Being a two particle operator the SMS is very sensitive to correlation effects, and its calculation is a challenge for atomic theory. The development of methods to include all-order correlation effects on the SMS is in progress, but to our knowledge no calculation has yet been performed for a many-electron system. Inclusion of the lowest-order correlation terms in atomic many-body perturbation theory has been found to give a significant—albeit insufficient—improvement in several cases [5–7] and is here applied to the electron affinity of chlorine, as described in section 3.

Since electron correlation is of major importance both for negative ions and for the specific mass shift, it would be of particular interest to investigate the specific mass shift in negative ions. However, the only one experiment, so far, where an isotope effect has been studied in an atomic negative ion is the measurement by Lykke et al. [8] of the electron affinities of hydrogen and deuterium. For these light systems the mass shift is, of course, very large, which enabled Lykke et al. to observe a shift, although the outgoing electron is a p wave, resulting in a slow onset of the photodetachment process. The main reason for the lack of studies of isotope shifts in negative ions is the absence of bound excited states which are optically accessible. The only sharp struc-

ture in an optical spectrum in the onset of the photodetachment process, and for most negative ions, this threshold is in a wavelength region not accessible to tunable dye lasers. Schulz et al. [9] have applied high-resolution techniques to study isotope effects in the negative *molecular* ions  $\text{OH}^-$  and  $\text{OD}^-$ , where, however, the major part of the mass effect is due to vibration and rotation and not from the electronic part, as in the case of atomic systems.

This work presents an investigation of the isotope shift of chlorine, which was chosen for several reasons. From an experimental point of view, Cl has the advantage, shared with all halogens, that an s electron is emitted in the photodetachment, giving a sharp threshold. In addition, it has two stable isotopes with large natural abundances. From a theoretical point of view, the closed-shell ground state of a halogen ion provides a convenient reference state for the calculations, and makes the system relatively easy to treat. In addition, the specific mass shift in the ionization potential of rare gases, which involve the same electron configuration, have been previously investigated, theoretically as well as experimentally [10–12], and the comparison of results can give an indication about the importance of various effects.

## 2 Experimental procedure and results

The experimental setup, shown in figure 1, has been described previously by Hanstorp and Gustafsson in connection with a similar experiment where the electron affinity of iodine was determined [13]. In this experiment, negative chlorine ions were formed from HCl gas on a hot  $\text{LaB}_6$  surface. The ions were accelerated to 3 keV, mass se-

lected in a sector magnet and focused by means of several Einzel lenses. In an analyzing chamber, the ions were merged with a laser beam between two electrostatic quadrupole deflectors placed 50 cm apart. An ion current of typically 6 nA for  $^{35}\text{Cl}$  and 2 nA for  $^{37}\text{Cl}$  was measured with a Faraday cup placed after the second quadrupole deflector. The laser light could be directed either parallel or antiparallel with respect to the ion beam direction. Fast neutral atoms produced in the photodetachment process were not affected by the second quadrupole deflector. Instead, they impinge on a glass plate coated with a conducting layer of tin doped indium oxide ( $\text{In}_2\text{O}_3:\text{Sn}$ ). Secondary electrons produced by the neutral atoms were collected with a channel electron multiplier (CEM) operating in pulse counting mode. The CEM was carefully shielded, both mechanically and electrically, to prevent stray electrons from reaching the detector [14].

An excimer pumped dye laser served as light source. The experiment was done using two different laser dyes BMQ (Lambdachrome No. 3570) and PTP (Lambdachrome No. 3400), with their peak intensities at 343 nm and 357 nm respectively. The laser pulses, with a time duration of 20 ns, had an energy of up to 1 mJ as measured in front of the experimental chamber. Some of the laser light was directed through as Fabry Perot etalon and through an acetylene-air flame for wavelength calibration.

## 2.1 Detection of the photodetachment threshold

According to the Wigner law [15], the cross section for photodetachment of an s wave electron is, in the vicinity of the threshold,

given by the expression

$$\sigma(E) = \begin{cases} c\sqrt{E - E_0}, & E \geq E_0 \\ 0, & E < E_0 \end{cases},$$

where  $\sigma(E)$  is the cross section for photodetachment,  $E$  is the photon energy,  $E_0$  is the photodetachment threshold, and  $c$  is a constant. The cross section behaviour is, however, complicated by the hyperfine structure. The two chlorine isotopes both have a nuclear spin of  $\frac{3}{2}$ . The ground state of the chlorine atom, which has the configuration  $3p^5\ ^2P_{3/2}$ , is therefore split into four hyperfine structure levels  $F = 0, 1, 2, 3$ , where the  $F = 0$  level has the lowest energy. The ground state configuration of the negative chlorine ion,  $3p^6\ ^1S_0$ , shows neither fine nor hyperfine structure. With one initial state and four possible final states there are four independent photodetachment channels, which all have to be included in the fitting procedure. The relative cross section for the different channels is proportional to the multiplicity of the final state in the neutral atom, i. e., proportional to  $2F + 1$ , and the total photodetachment threshold can therefore be described by the function

$$\sigma(E) = c \sum_{F=0}^3 (2F + 1) \times \sqrt{E - (E_0 + E_{\text{hfs}}^F)}, \quad E \geq E_0$$

where  $E_{\text{hfs}}^F$  is the  $F$  dependent energy correction due to the hyperfine interaction [16],  $E_0$  the threshold energy for leaving the atom in the lowest hyperfine level of the ground state of the atom, and  $c$  is a constant.

The nonzero bandwidth  $B$  of the laser also has to be taken into account in the evaluation procedure. In our case, we can assume a Gaussian intensity distribution

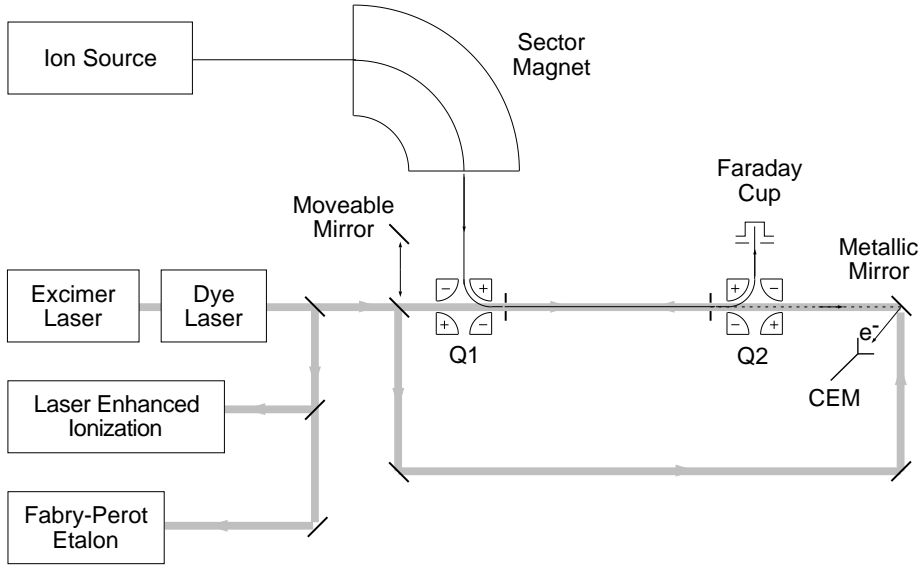


Figure 1: *Experimental setup.*

$I(E')$  with its peak at  $E' = 0$  given by the expression [17]

$$I(E') = \frac{e^{-4(E'/B)^2}}{2} .$$

Including this bandwidth into the fitting procedure, the experimental values can be fitted to the following modified Wigner law function:

$$\begin{aligned} \sigma(E) = C & \int_{E'=-\infty}^{\infty} \sum_{F=0}^3 I(E')(2F+1) \\ & \times \left\{ \left[ E + E' - (E_0 + E_{\text{hfs}}^F) \right] \right. \\ & \left. + \left| E + E' - (E_0 + E_{\text{hfs}}^F) \right| \right\}^{1/2} dE' . \quad (1) \end{aligned}$$

The term inside the absolute sign is included in order to make the function equal to zero below the threshold. The experimental data points were fitted to equation (1) using a nonlinear fitting routine based on the Levenberg-Marquardt method [18]. An example of such a fit is shown in figure

2. Although equation (1) is complicated, only the constant  $C$  and the threshold energy  $E_0$  are varied to fit the data. The two Fabry Perot peaks closest to the threshold, shown in the upper part of figure 2, were fitted to an Airy function by the same numerical method, and their position served as frequency markers.

To determine the laser bandwidth, the expression in equation (1) was fitted to one set of experimental data for different values of the laser bandwidth. The standard deviation of those fits varied smoothly with energy, with a minimum at a bandwidth of 4.3 GHz. This value agrees with the laser specification and was used for all subsequent evaluations.

In order to correct for the first-order Doppler shift, which is sufficient in this experiment, the electron affinity  $E_{\text{EA}}(^A\text{CL})$  of the isotope  $^A\text{CL}$  is obtained as average value of the energy of the photodetachment threshold,  $E_{\text{th}}$  obtained with parallel and antiparallel laser and ion beams (des-

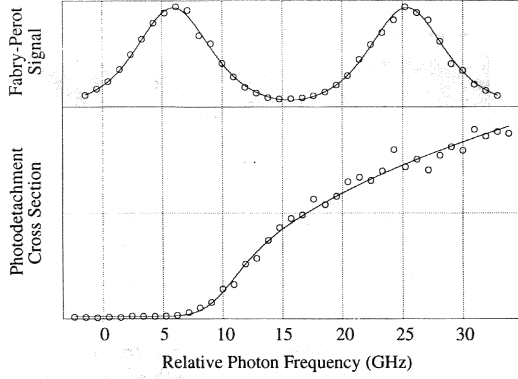


Figure 2: A scan used in the isotope-shift measurement. The lower curve is the relative cross section for photodetachment where the line is a fit to the experimental data. The upper curve is the transmission through a Fabry-Perot etalon used for frequency calibration.

ignated p and a, respectively):

$$E_{\text{EA}}(A\text{CL}) = \frac{E_{\text{th}}^{\text{a}} + E_{\text{th}}^{\text{p}}}{2} \quad (2)$$

## 2.2 Isotope shift

The isotope shift of the electron affinity in the negative chlorine ion has been experimentally determined by measuring the difference in electron affinity for the two stable chlorine isotopes, each determined as described in section 2.1.

The frequency shift corresponding to the difference in electron affinity, as shown in figure 3, is given by the equation

$$\Delta E_{\text{EA}} = E_{\text{EA}}(^{37}\text{CL}) - E_{\text{EA}}(^{35}\text{CL}) \quad (3)$$

Alternatively, this shift can be obtained by combining equations (2) and (3) giving the

expression

$$\begin{aligned} \Delta E_{\text{EA}} &= \frac{E_{\text{th}}^{\text{a}} - E_{\text{th}}^{\text{p}}}{2} \\ &= \frac{E_{\text{th}}^{\text{a}}(^{37}\text{CL}) - E_{\text{th}}^{\text{a}}(^{35}\text{CL})}{2} \\ &\quad - \frac{E_{\text{th}}^{\text{p}}(^{35}\text{CL}) - E_{\text{th}}^{\text{p}}(^{37}\text{CL})}{2} \end{aligned}$$

Experimentally, this has the advantage that two pairs of thresholds situated very close to each other are compared, making the laser scans much shorter.

Four threshold measurements are thus required for one determination of the difference in the electron affinities of the two isotopes,  $\Delta E_{\text{EA}}$ . In the present work, we present a total of 13 isotope shift determinations, giving an experimental value

$$\frac{\Delta E_{\text{EA}}}{h} = 0.34(14)\text{GHz} \quad (4)$$

Since the experimental results are obtained by comparing the energy of different thresholds, they are independent of an absolute wavelength calibration. Many systematic effects will therefore cancel in the evaluation procedure, giving a very high accuracy of the experimental result.

The electron affinity is defined from the threshold energy, and thus involves the difference between the ground state of the negative ion and the lowest hyperfine level of the ground state atom, whereas the isotope shift is normally defined as the difference between the fine-structure levels unperturbed by the hyperfine interaction. In order to extract the isotope shift from the experimental shift  $\Delta E_{\text{EA}}$  in equation (4), it is necessary to correct for the energy difference,  $\Delta E_{\text{hfs}}^F = h\delta\nu_{\text{hfs}}^F$ , between the lowest hyperfine-structure level of the Cl atom and the fine-structure level unperturbed by the hyperfine structure. In  $^{35}\text{Cl}$ ,

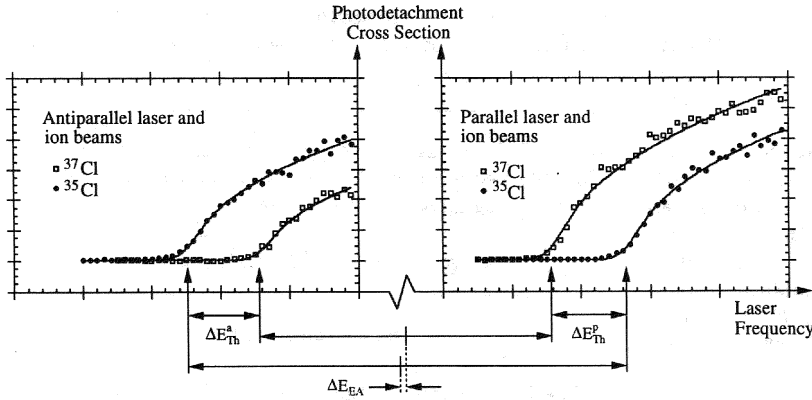


Figure 3: A graphic description of the evaluation of the isotope shift from four different experimentally determined photodetachment thresholds.

the  $F = 0$  ground-state level is situated  $\delta\nu_{\text{hfs}}^F(^{35}\text{Cl}) = 0.700$  GHz below the unperturbed level and the corresponding shift in  $^{37}\text{Cl}$  is  $\delta\nu_{\text{hfs}}^F(^{37}\text{Cl}) = 0.586$  GHz. These shifts are illustrated in figure 4 and were obtained using the Casimir formula, where the  $A$  and  $B$  hyperfine constants were taken from Fuller [16]. Subtracting the difference between these two values from  $\Delta E_{\text{EA}}$  gives a corrected isotope shift of the electron affinity of Cl:

$$\begin{aligned} \delta\nu_{\text{IS}} &= \frac{\Delta E_{\text{EA}}}{h} + \delta\nu_{\text{hfs}}^F(^{37}\text{Cl}) - \delta\nu_{\text{hfs}}^F(^{35}\text{Cl}) \\ &= 0.22(14) \text{ GHz} \quad . \end{aligned} \quad (5)$$

### 2.3 Electron affinity

In addition to the isotope-shift measurements, an improved absolute value of the electron affinity of  $^{35}\text{Cl}$  has been determined. Extended descriptions of the experimental procedure for this experiment has been given elsewhere [13,19].

The laser wavelength was scanned between 343.7...344.7 nm in steps of 0.0005 nm. At each wavelength the signal from 30 laser pulses were averaged. In total seven scans, one of which is shown in figure 5, were recorded. Three different

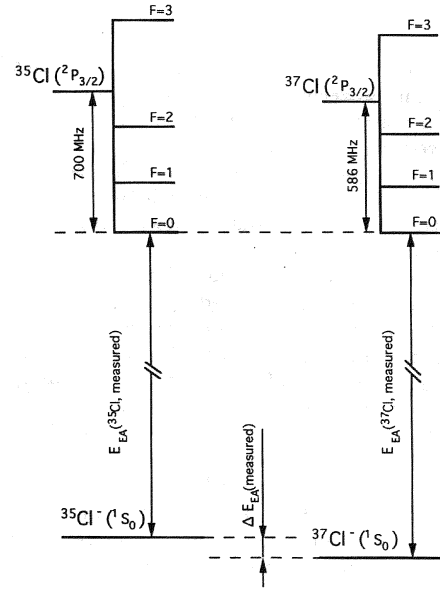


Figure 4: The energy level diagram of the ground state of  $\text{Cl}^-$  and  $\text{Cl}$ . The zero energy is set to the lowest hyperfine level in the atomic ground state of the two isotopes.

signals were registered, namely, the number of atoms neutralized in the photodetachment process, laser enhanced ionization of nickel in an acetylene-air flame [20], and the transmission through a Fabry Perot etalon. The direction of the laser beam was reversed in the middle of the scans in order to acquire the threshold position

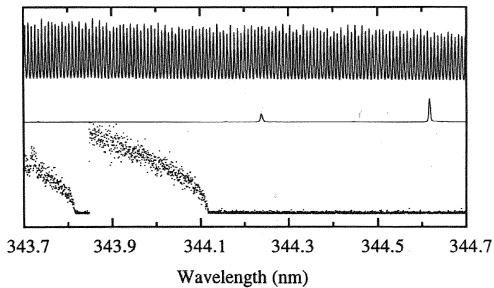


Figure 5: A complete recording of a spectrum used for determination of the electron affinity. The lower curve is the relative cross section, the middle curve is laser-enhanced ionization of nickel in a flame, and the upper curve is the transmission through a Fabry-Perot étalon. The direction of the laser beam was reversed at approximately 343.85 nm.

for both the parallel and the antiparallel laser-ion beam geometries in each scan. The threshold positions were evaluated using the method described in section 2.1. The resonant absorption lines in nickel were fitted to Lorentzian functions in order to find their peak positions. The Fabry Perot etalon fringes served as frequency markers in order to connect the threshold energies with the reference lines. The electron affinity, corrected for the Doppler shift, was determined by taking the mean value of the energies for the parallel and antiparallel photodetachment thresholds, as shown in equation (2).

The energies of the nickel reference lines have recently been measured using Fourier-transform spectroscopy [21], and they are known to within  $10^{-3} \text{ cm}^{-1}$ . As previously mentioned, we use laser-enhanced ionization in a flame in order to detect these lines [20]. The main sources of uncertainty in our calibration procedure are broadening and shifts caused by collisions in the

flame. Spectral lines are at the most redshifted with 1/3 of the pressure broadening, and experimentally observed shifts are normally smaller [22]. The widths of the spectral line profiles that we observed were approximately 11 GHz. When the contribution from the laser bandwidth and the Doppler broadening has been taken into account, a remaining pressure broadening of 10 GHz was obtained. We therefore estimate the redshift of our reference lines to be smaller than 3.3 GHz. Isotope shifts of the nickel reference lines have been measured [23] but are too small to influence our measurements.

The statistical scattering in this measurement is only  $0.013 \text{ cm}^{-1}$ . This corresponds to 0.4 GHz, which is less than one tenth of the laser bandwidth. In the error in our final result of the electron affinity, we include two standard deviations of the statistical uncertainty plus the maximum possible systematic shift due to the calibration procedure. This results in an electron affinity of

$$\frac{E_{\text{EA}}}{hc} = 29\,138.59(22) \text{ cm}^{-1} ,$$

which is within the uncertainty of the previously reported most accurate value  $29\,138.3(5) \text{ cm}^{-1}$  [24], and an improvement of the accuracy with a factor of two. Further, it is within the uncertainty of the result of  $29\,138.9(7) \text{ cm}^{-1}$  which we recently reported [19]. In the present investigation, we have used more accurately known atomic reference lines which lie closer to the photodetachment thresholds, and we have improved the statistics. The Ni reference lines used in the investigations are  $(3d^8 4s^2 \ ^3F_4 \mapsto 3d^8 4s 4p \ ^5F_4)$  at  $29\,084.455(1) \text{ cm}^{-1}$  and  $(3d^9 4s \ ^3D_3 \mapsto 3d^9 4p \ ^3F_3)$  at  $29\,115.975(1) \text{ cm}^{-1}$ . All these values of the electron affinity of chlo-

rine agree within their uncertainties, but they are outside the error bars of the value of  $29\,173(24)\text{ cm}^{-1}$  recommended by Hoptop and Lineberger in their compilation of atomic electron affinities [25]. With three additional determinations of the electron affinity of chlorine, it should be possible to give a more accurate recommended value.

### 3 Isotope shift calculations

The different nuclear masses and charge distribution of  $^{35}\text{Cl}$  and  $^{37}\text{Cl}$  leads to a shift in the electron affinity which can be written as [26]

$$\delta\nu_i^{A,A'} = K_i^{\text{MS}} \frac{M_A - M_{A'}}{(M_{A'} + m_e)M_A} + F_i(1 - \kappa)\delta\langle r^2 \rangle^{A,A'} \quad (6)$$

where the first term is the mass shift accounting for the nuclear motion and the second term is the field shift arising from the change in electrostatic potential from the nucleus due to the change in charge distribution. For light elements, like Cl, the mass shift dominates. It falls off rapidly with the nuclear mass, whereas the field shift increases for heavy elements, since the orbitals become more and more contracted and the nucleus more extended. The small correction for the field isotope shift is discussed in section 3.2.

The expression for the mass shift factor is found by expanding the nuclear kinetic energy in equation (6) as

$$\begin{aligned} \frac{\mathbf{P}_N^2}{2M_A} &= \frac{(\sum_i \mathbf{p}_i)^2}{2M_A} \\ &= \frac{\sum_i \mathbf{p}_i^2 + \sum_{i \neq j} \mathbf{p}_i \cdot \mathbf{p}_j}{2M_A} \end{aligned}$$

We find that the mass shift factor can be divided into two terms,

$$K^{\text{MS}} = K^{\text{NMS}} + K^{\text{SMS}}$$

where the first term

$$K^{\text{NMS}} = m_e \nu$$

gives the “normal” mass shift, and accounts for the effect of substituting the electron mass

$$m_e = 5.4858 \times 10^{-4} \text{ u}$$

by the reduced mass

$$\mu = \frac{m_e M}{m_e + M}$$

in the Schrödinger equation. For the electron affinity of Cl,

$$K^{\text{NMS}} = 479.43 \text{ GHz u} \quad .$$

The mass shift between the two Cl isotopes is obtained by multiplication of the mass shift factor,  $K^{\text{MS}}$ , with the mass factor

$$\frac{M_{37} - M_{35}}{M_{35}(M_{37} + m_e)} \approx 0.00155 \text{ u}^{-1} \quad ,$$

giving

$$\delta\nu^{\text{NMS}} = 0.74 \text{ GHz} \quad .$$

The nuclear masses

$$M_{35} = 34.96 \text{ u}$$

and

$$M_{37} = 36.96 \text{ u}$$

are obtained by subtracting  $17 m_e$  from the atomic masses.

The second part,

$$K^{\text{SMS}} = \frac{\Delta\langle \sum_{i \neq j} \mathbf{p}_i \cdot \mathbf{p}_j \rangle}{h} \quad ,$$

involves two electrons simultaneously and describes a correlation between the electronic momenta arising through the motion of the nucleus. Here, we use this non-relativistic operator, although the orbitals



used for the evaluation were obtained relativistically. The theoretical results are presented in terms of  $K^{\text{SMS}}$  in order to facilitate comparison between results for different elements.

### 3.1 The specific mass shift

The observable shift in the electron affinity results from the change in this expectation value between the closed shell ground state of  $\text{Cl}^-$  and the ground state of the neutral system with its  $3p_{3/2}$  hole. This can be described using essentially the same formalism as developed for systems with one valence electron outside a closed shell, although the correlation between a hole and the core tends to be more important. In this work, however, we have included only lowest order correlation effects, using direct summation of numerical relativistic basis functions obtained using the methods described by Salomonson and Öster [27]. This method has been applied to SMS calculations for Cs, Tl [7], and  $\text{Yb}^+$  [28] and the generalization to a hole follows that used in the nonrelativistic calculation for the shift of the binding energy of Ne [6].

For scalar operators, like the SMS, the core gives very large contributions ( $\approx -144$  THz u in this case), which, however, cancel between initial and final states. An advantage of perturbation theory is the cancellation of contributions from the unperturbed core automatically obtained by omitting the “zero-body” terms describing these contributions. In the case of a single hole state only “one-body” terms need to be evaluated.

The first contribution to  $K^{\text{SMS}}$  is the interaction of the hole with all core electrons. Only the exchange terms contribute to the expectation value, making the first-order value negative. Evaluating the ex-

pectation value between Dirac-Fock (DF) orbitals for the ground state of  $\text{Cl}^-$ , which is used as a reference, gives  $-3.68$  THz u. The DF value is a sum over the interactions of the  $3p_{3/2}$  with all core orbitals whose  $l$ -quantum number differs by one unit and  $j$  value differs by at most one unit from the value of the hole, i.e., all the  $ns$  electrons. The interaction with  $1s$  electrons is found to dominate, giving  $-2.24$  GHz u—the smaller overlap is compensated by the larger momenta of the inner core electrons.

The ionization of Ne, studied in earlier work [6], involves the removal of a  $2p_{3/2}$  electron. In that case, the DF contribution to the mass shift constant,  $K^{\text{SMS}}$ , is  $-9.00$  THz u, of which the  $1s$ - $2p$  interaction accounts for  $-8.24$  THz u. In spite of the larger nuclear charge of Cl, which leads to increased electronic momenta, the higher principal number of the active electron in Cl leads to a smaller DF value for  $K^{\text{SMS}}$ .

The nuclearmotion affects the wave function of *all* electrons, thereby modifying, e.g., the interaction between the core and the  $3p$  hole. The change in the  $3p$  energy due to the first-order correction of the core gives a contribution  $4.77$  THz u to the SMS constant, i.e., larger than the DF value but with opposite sign. However, these orbital corrections affect also the interactions within the core. A self-consistent treatment of the core orbital modifications, closely related to the “random-phase approximation” (RPA) approach, reduces the orbital modification effect by about 40 %, to  $2.83$  THz u. Adding this value to the DF contribution cancels a large part of it, leaving a sum of only  $-0.84$  THz u. We note that Bauche [29], in his pioneering nonrelativistic isotope-shift calculations, performed separate Hartree-Fock calculations for the initial and final states and in this way include automatically the

“RPA” terms. Also for the shift of the ionization energy in Ne, the orbital modifications give significant reduction of the mass shift constant, although the corrections for an atom are not quite as drastic as for a negative ion, where the interaction between the electrons plays a more dominant role. The first-order modification gives 8.72 THz u, changed to 5.43 THz u by the self-consistent treatment. Figure 6 shows the theoretical results at different levels of approximation for these systems, together with the experimental values. Being a two-particle operator the SMS is very sensitive to correlation effects, which arise already in second order where they were found to give 1.7 THz u, thereby changing the overall sign, giving

$$K^{\text{SMS}} = 0.32 \text{ THz u}$$

corresponding to a shift between the two stable Cl isotopes of 0.50 GHz. In view of the large cancellations, this result is very uncertain. For Ne, the lowest-order correlation effect, 2.04 THz u, leads to a theoretical value  $-1.54$  THz u, compared to the experimental value  $-2.4$  THz u. Higher-order effects must thus reduce the correlation contribution for Ne. Lowest-order correlation effects, in fact, often give an overestimate, as pointed out by Dzuba et al. [30], who advocate the use of a screened Coulomb potential to describe the electron correlation. The modification of the valence orbital to an approximate Brueckner orbital is often a very important correlation effect [31]. Here, we evaluated these corrections to the lowest order, and found a reduction of the DF and RPA results of only about 1.4 %. A more complete treatment of higher-order correlation effects would be essential to obtain agreement with experimental data.

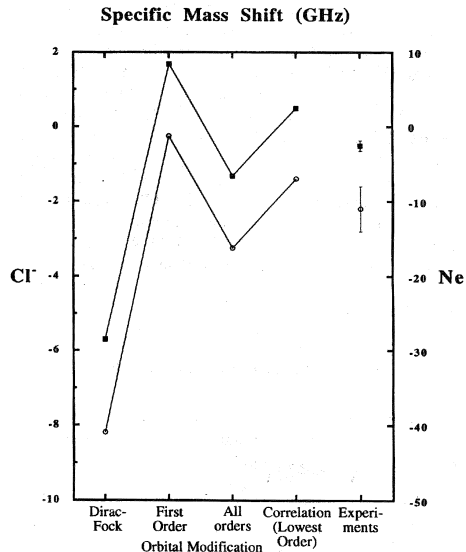


Figure 6: A comparison between the experimental value for the specific mass shift for the electron affinity in Cl and theoretical results at different levels of approximation. For comparison, the corresponding results are also shown for the shift of the ionization potential of Ne (with the scale to the right). The first value is evaluated using orbitals obtained in the Dirac-Fock potential from the unperturbed closed-shell core and the next two values show, respectively, the lowest-order and all-order effect of the modification of the core orbitals due to the removal of an  $np$  electron. The final theoretical value accounts also to lowest (i.e., second) order for the correlation effects and involves the simultaneous excitation of two electrons (GHz).

### 3.2 The field isotope shift

In addition to the mass-dependent isotope shift described above, a shift in the electron affinity can also arise due to changes  $\delta\langle r^2 \rangle^{35:37}$  in the nuclear charge distribution, as shown in equation (6). The electronic factor  $F$  for the field shift is given by

$$F = -4\pi\Delta|\Psi(0)|^2 \frac{Z}{6} \frac{q_e^2}{4\pi\epsilon_0}$$

and is determined by the change in electron density,  $|\Psi(0)|^2$ , at the nucleus between the lower and upper state of the transition. The  $3p_{3/2}$  electron, itself, has a negligible density at the nucleus. Nevertheless, its removal causes a change in the distribution of the s electrons in the core. Including the RPA-type corrections to first order gives

$$F \approx 254 \text{ MHz/fm}^2 \quad .$$

Similar to the SMS, a self-consistent treatment of the RPA terms gives a significant reduction:

$$F \approx 117 \text{ MHz/fm}^2 \quad .$$

We note that this value is comparable to the factor

$$F_{4s}(K) \approx -103 \text{ MHz/fm}^2$$

for the binding energy of the 4s ground state of the nearby alkali-metal K, but is considerable larger than the factor for its first p state

$$F_{4p} \approx 4.6 \text{ MHz/fm}^2 \quad .$$

The correction term  $\kappa$  in equation (6) accounts for higher moments,  $\delta\langle r^4 \rangle$ ,  $\delta\langle r^6 \rangle$ ,  $\dots$ , of the nuclear charge distribution, but is negligibly small (about 0.4%) for Cl.

Briscoe et al. [32] have measured the charge distribution of  $^{35}\text{Cl}$  and  $^{37}\text{Cl}$ . using electron scattering. From their parameters for the Fermi distribution, we obtain

$$\delta\langle r^2 \rangle^{35:37} = 0.12(12) \text{ fm}^2 \quad .$$

Combining this result with our calculated  $F$  value indicates that the field isotope shift of the electron affinity

$$\delta\nu_{\text{FS}}^{35:37} = 14(14) \text{ MHz} \quad ,$$

which is well below the error bars of the isotope shift measurement.

## 4 Comparison between theory and experiment

The experimentally determined difference between electron affinity for the naturally occurring chlorine isotopes of the fine structure levels unperturbed by the hyperfine interaction was  $\Delta\nu_{\text{IS}} = 0.22(14)$  MHz, as discussed in section 2.2.

Subtraction of the normal mass shift (see section 3)

$$\delta\nu_{\text{NMS}} = \frac{\nu m_e \Delta M}{M_{35} M_{37}} = 0.74 \text{ GHz}$$

give a “residual shift” of  $-0.51(14)$  GHz. As seen in section 3.2, the field shift is only

$$\delta\nu_{\text{FS}} = 14(14) \text{ MHz} \quad ,$$

leaving a specific mass shift of

$$\delta\nu_{\text{SMS}} = -0.51(14) \text{ GHz}$$

corresponding to a factor

$$K_{\text{SMS}} = -0.33(9) \text{ THz u} \quad .$$

This value is close to the theoretical result, but with opposite sign.

In order to understand better the cause of this apparent contradiction, we show in figure 6 the results obtained at various levels of approximation. The final result arises from large cancellation. The DF expectation value is many times larger than the final result. The lowest-order orbital modification (“RPA terms”) is of comparable size and with opposite sign. Higher-order RPA terms cancel about 40% of the lowest-order orbital modification correction. It seems like the lowest-order correlation effects are overestimated by a similar amount: the experimental value is about halfway between the result with and without lowest-order correlation. For comparison we shown in figure 6 also the experimental [12] and analogous theoretical values [6] for the specific

mass shift in the ionization potential of neon. The calculated specific mass shift for neon is  $-7$  GHz, whereas the experimental value is  $-11.3$  GHz. Although slightly outside the uncertainty of the experimental value, the theoretical value in this case has the right sign. The negative first-order DF value plays a more dominant role for an atom than for a negative ion.

Similar results are obtained for the chlorine electron affinity, itself: The DF value,  $0.1480$  a.u., is about 11% larger than the experimental value  $0.1328$  a.u., but the lowest-order correlation effects bring a reduction of about 20%, giving a theoretical value of  $0.1181$  a.u., again demonstrating the need of more complete treatment of correlation effects. The coupled-cluster approach provides a systematic procedure for including higher-order effects [33], which has given quite accurate results for systems with one valence electron [34], and could be applied also to hole states, although that has not yet been implemented in our program.

## 5 Conclusion

We have determined the isotope shift in the electron affinity of Cl to be  $0.22(14)$  GHz, of which  $-0.51(14)$  GHz is due to the specific mass shift. This is to our knowledge the highest resolution obtained in any laser experiment on atomic negative ions, and the resolution is even higher than in electron affinity determinations where single-mode dye lasers have been used [35]. This could be achieved since an isotope-shift measurement involves comparison of photodetachment thresholds, rather than absolute determination. Many systematic uncertainties will therefore cancel, giving a very high accuracy in the experimental re-

sult. Further, the collinear geometry with the high photon flux from the pulsed dye lasers gives very good counting statistics.

Experimentally it would be very hard to improve the resolution on the isotope shift on chlorine since the measured shift is only  $1/30$  of the bandwidth of the laser. A more precise experiment could, however, be made using a negative ion where the photodetachment threshold corresponds to the wavelength region of a single-mode dye laser. The laser light should then be amplified in a pulsed amplifier in order to keep the good signal to background ratio obtained in the present experiment.  $S^-$  could then be a suitable choice, although it would probably be necessary to use isotopically enriched sulfur. The theoretical treatment of such a system is more complicated, but might be amenable to multiconfiguration Hartree-Fock calculation [36, 37]. Investigating a few-electron system, like  $Li^-$ , would give more insight, since very accurate calculations could be performed. In this case, however, the experimental conditions are much more unfavorable. Nevertheless, the experimental accuracy in the shift of the electron affinity of Cl is sufficient to demonstrate the importance of higher-order correlation effects.

Finally, we conclude that this is the third experiment showing an electron affinity of chlorine deviating from the currently recommended value. A more precise recommendation of this quantity could therefore be given by means of this and previous experiments.

## Acknowledgements

We would like to express our appreciation to Ove Axner, who lent us the laser system used in the experiment. Financial sup-

port by the Swedish Natural Science Research Council is gratefully acknowledged. The visit by Uldis Berzinsh was made possible by financial support from the Swedish Institute and from the International Research Fund at Göteborg University.

## References

- [1] Sten Salomonson and Per Öster. Numerical solution of the coupled-cluster single- and double-excitation equations with application to Be and  $\text{Li}^-$ . *Phys. Rev. A*, 41(9):4670–4681, May 1990.
- [2] S. Geltman. Multiphoton detachment of an electron from  $\text{H}^-$ . *Phys. Rev. A*, 42:6958–6961, 1990.
- [3] M. L. Du. Photodetachment spectra of  $\text{H}^-$  in parallel electric and magnetic fields. *Phys. Rev. A*, 40:1330–1339, 1989.
- [4] M. Vincke and D. Baye. Variational study of  $\text{H}^-$  and He in strong magnetic fields. *J. of Phys. B: At., Mol. Opt.*, 22:2089–2102, 1989.
- [5] A.-M. Mårtensson and S. Salomonson. Specific mass shifts in Li and K calculated using many-body perturbation theory. *J. of Phys. B: At. and Mol.*, 15:2115–2130, 1982.
- [6] S. Hörbäck, A.-M. Mårtensson-Pendrill, S. Salomonson, and U. Österberg. The specific mass shift of the ionisation energy in Ne calculated by many-body perturbation theory. *Phys. Scr.*, 28:469–471, 1983.
- [7] A. Hartley and A.-M. Mårtensson-Pendrill. Calculations of isotope shifts in caesium and thallium using many-body perturbation theory. *J. of Phys. B: At., Mol. Opt.*, 24(6):1193–1207, March 1991.
- [8] K. R. Lykke, K. K. Murray, and W. C. Lineberger. Threshold photodetachment of  $\text{H}^-$ . *Phys. Rev. A*, 43(11):6104–6107, June 1991.
- [9] P. A. Schulz, R. D. Mead, P. L. Jones, and W. C. Lineberger.  $\text{OH}^-$  and  $\text{OD}^-$  threshold photodetachment. *J. Chem. Phys.*, 77:1153–1165, 1982.
- [10] G. Herzberg, F.R.S. Ionization potentials and Lamb shifts of the ground states of  $^4\text{He}$  and  $^3\text{He}$ . *Proc. R. Soc. London, Ser. A*, 248(1254), November 1958.
- [11] S. A. Aseyev, Y. A. Kudryavtsev, V. S. Letokhov, and V. V. Petrunin. A method of detecting the rare isotopes  $^{85}\text{Kr}$  and  $^{81}\text{Kr}$  by means of collinear laser photoionization of atoms in an accelerated beam. *J. of Phys. B: At., Mol. Opt.*, 24(11):2755–2763, 1991.
- [12] W. B. Westerveld and J. van Eck. Isotope shift between the ground level of  $^{20}\text{Ne}$  and  $^{22}\text{Ne}$ . *J. of Phys. B: At., Mol. Opt.*, 12:377–381, 1979.
- [13] D. Hanstorp and M. Gustafsson. Determination of the electron affinity of iodine. *J. of Phys. B: At., Mol. Opt.*, 25:1773–1783, 1992.
- [14] D. Hanstorp. A secondary emission detector capable of preventing detection of the photoelectric effect induced by pulsed lasers. *Meas. Sci. Technol.*, 3:523–527, 1992.

- [15] Eugene P. Wigner. On the behavior of cross sections near thresholds. *Phys. Rev.*, 73(9):1002–1009, 1948.
- [16] G. H. Fuller. Nuclear spins and moments. *J. Comput. Phys.*, 5:835–920, 1976.
- [17] Walter Demtröder. *Laserspektroskopie*. Springer Verlag, third edition, 1988.
- [18] W. H. Press, B. P. Flannery, S. A. Teukolsky, and W. T. Vetterling. *Numerical Recipes. The Art of Scientific Computing (FORTRAN Version)*. Cambridge University Press, Cambridge, 1989.
- [19] D. Hanstorp, M. Gustafsson, U. Berzinsh, and U. Ljungblad. Collinear photodetachment spectroscopy. *Nucl. Instrum. Methods*, 79:159–161, 1993.
- [20] O. Axner, T. Berglind, J. L. Heully, I. Lindgren, and H. Rubinsztein-Dunlop. Improved theory of laser-enhanced ionization in flames: Comparison with experiment. *J. Appl. Phys.*, 55(9):3215–3225, May 1984.
- [21] Ulf Litzén, Brault James W, and Anne P. Thorne. Spectrum and term system of neutral nickel, Ni I. *Phys. Scr.*, 47(5):628–673, May 1993.
- [22] H. C. Wagenaar and L. de Galan. Interferometric measurements of atomic line profiles emitted by hollow-cathode lamps by an acetylene-nitrous oxide flames. *Spectrochim. Acta B*, 28:157–177, 1973.
- [23] D. J. Schroeder and J. E. Mack. Isotope shift in the arc spectrum of Nickel. *Phys. Rev.*, 121(6):1726–1731, March 1961.
- [24] R. Trainham, G. D. Fletcher, and D. J. Larson. One- and two-photon detachment of the negative chlorine ion. *J. of Phys. B*, 20:L777–L784, December 1987.
- [25] H. Hotop and W. C. Lineberger. Binding energies in atomic negative ions. *J. Phys. Chem. Ref. Data*, 14(3):731–750, 1985.
- [26] W. H. King. *Isotope shifts in atomic spectra*. Plenum Press, New York and London, 233 Spring street, New York, N.Y. 10 013, 1984.
- [27] S. Salomonson and P. Öster. Solutions of the pair equation using a finite discrete spectrum. *Phys. Rev. A*, 40(10):5559–5567, 1989.
- [28] Ann-Marie Mårtensson-Pendrill, David S. Gough, and Peter Hannaford. Isotope shifts and hyperfine structure in the 369.4 nm  $6s-6p_{1/2}$  resonance line of singly ionized ytterbium. *Phys. Rev. A*, 49(5):3351–3365, May 1994.
- [29] J. Bauche. Hartree-Fock evaluations of specific mass isotope shifts. *J. Physq.*, 35(1):19–26, January 1974.
- [30] V. A. Dzuba, V. V. Flambaum, P. G. Silvestrov, and O. P. Sushkov. Screening of Coulomb interaction and many-body perturbation theory in atoms. *Phys. Lett. A*, 131(7,8):461–465, September 1988.

- [31] Ingvar Lindgren, Johannes Lindgren, and Ann-Marie Mårtensson. Many-body calculations of hyperfine interaction of some excited states of alkali atoms, using approximate Brueckner natural orbits. *Z. Phys. A*, 279:113–125, 1976.
- [32] W. J. Briscoe, Hall Crannell, and J. C. Bergstrom. Elastic electron scattering from the isotopes  $^{35}\text{Cl}$  and  $^{37}\text{Cl}^*$ . *Nucl. Phys. A*, 344:475–488, 1980.
- [33] Ingvar Lindgren. A coupled-cluster approach to the many-body perturbation theory for open-shell systems. In Per-Olov Löwdin and Yngve Öhrn, editors, *Atomic, molecular, and solid-state theory, collision phenomena, and computational methods*, volume 12 of *International Journal of Quantum Chemistry, Quantum Chemistry Symposium*, pages 33–58. John Wiley & Sons, March 1978.
- [34] Sten Salomonson and Anders Ynnerman. Coupled-cluster calculation of matrix elements and ionization energies of low-lying states in sodium. *Phys. Rev. A*, 43(1):88–94, January 1991.
- [35] D. M. Neumark, K. R. Lykke, T. Andersen, and W. C. Lineberger. Laser photodetachment measurement of the electron affinity of atomic oxygen. *Phys. Rev. A*, 32(3):1890–1892, September 1985.
- [36] Charlotte Froese Fischer. A general multi-configuration Hartree-Fock program. *Computer Phys. Comm.*, 64(3):431–454, June 1991.
- [37] H. A. Schuessler, A. Alousi, M. Idrees, Y. F. Li, F. Buchinger, R. M. Evans, and C. F. Fischer. Isotope shifts and hyperfine structure splitting constants of the 4d-5p transitions of Kr II at  $\lambda=729$  nm. *Phys. Rev. A*, 45(9):6459–6467, May 1992.